III International Conference on Particle-based Methods – Fundamentals and Applications
PARTICLES 2013
M. Bischoff, E. Oñate, D.R.J. Owen, E. Ramm & P. Wriggers (Eds)

MPS SIMULATION OF SPREADING BEHAVIOR OF MOLTEN MATERIALS

T.MATSUURA* AND Y. OKA

* Cooperative major in Nuclear Energy, Waseda University
3-4-1, Ohkubo, Shinjuku-ku, Tokyo 169-8555, Japan
E-mail: globe.of.fancy1t@suou.waseda.jp

Key words: MPS, core melt, severe accident, spreading, core catcher, solidification, FARO, ECOKATS

Abstract. Spreading behavior with solidification is important phenomenon for the assessment of containment integrity and managing the severe accident in nuclear power plants. Existing codes such as CORFLOW use empirical equations for analyzing spreading behavior. Moving particle semi-implicit (MPS) method which calculates free surface without empirical equations is suitable for analyzing the solidification behavior of fluid with large deformation.

MPS calculation models have been developed for the spreading analysis and deal with calculating thermal field, buoyancy, solid-liquid phase transition and temperature dependency of viscosity. The code was improved to calculate radiation heat transfer in three dimensions and high viscosity materials, and to control numerical instability. The FARO L26S and ECOKATS-V1 experiments were analyzed and showed good agreements with the experimental results in terms of final position of melt spread. Water Spreading Test by Theofanous and SPREAD test using stainless steel melt, were analyzed and compared with the results by SAMPSON code. Both analyses agreed with the experiments. The MPS method will be useful for computer experiments with various physical property of corium. It is expected to improve severe accident analysis code.

1 INTRODUCTION

Mitigation of core meltdown accident is important for reactor safety. For the purpose, it is important to analyze spreading behavior of molten core materials with solidification on the containment floor. That is because the spreading phenomenon is directly related to emission of radioactive materials caused by the damage to the shell of the containment vessel. The behavior also has an effect on the initial condition of molten core concrete interaction (MCCI) in the severe accident analysis, and designing a core catcher which is equipment for ex-vessel molten core retention.

In order to understand clearly the spreading behavior with solidification, several flow experiments using high temperature melts was conducted. One of them is the FARO experiment using a mixture of uranium dioxide (UO_2) and zirconium dioxide (ZrO_2) which was simulated molten core melt [1]. Others are the SPREAD and KATS experiments with an alumina mixture over 2000K. The CORFLOW, LAVA and THEMA codes are representatives of computer codes for analyzing these flow experiments. These codes are based on Eulerian methods. So they have difficulties of tracking free surface and calculating temperature profile

without empirical equations obtained from experiments [2,3].

Lagrangian methods are other approaches to overcome these problems. A moving particle semi-implicit (MPS) method is a deterministic Lagrangian method developed for calculating incompressible fluids [4]. In this method, computational grid is unnecessary and therefore, flow with free surface and phase change can be easily calculated without empirical equations. MPS calculation models had been developed for the spreading analysis and deals with calculating thermal field, buoyancy, solid-liquid phase transition and temperature dependence of viscosity. The FARO experiment was analyzed with the MPS method and compared with the experimental results [5]. But the analysis had difficulties of numerical instability for calculating high viscosity materials in a phase change area and cannot calculate a radiation heat transfer.

In this work, the MPS code was improved to calculate radiation heat transfer in three dimensions and high viscosity materials by the implicit viscosity calculation and to control numerical instability. Using the improved MPS code, FARO and ECOKATS-V1 experiments are analyzed for more accurate melt spreading behavior calculation. Water Spreading Test by Theofanous and SPREAD test which were used for validation of SAMPSON code are also analyzed and compared with the results by SAMPSON code.

2 NUMERICAL MODELS AND METHODS FOR MPS

2.1 Governing equation in MPS method

Governing equations for incompressible flows are mass, momentum and energy conservation equations as follows:

$$\frac{\partial \rho}{\partial t} = 0 \tag{1}$$

$$\frac{\partial \boldsymbol{u}}{\partial t} = -\frac{1}{\rho}\nabla P + \nu \nabla^2 \boldsymbol{u} + \boldsymbol{F} \tag{2}$$

$$\frac{\partial T}{\partial t} = \frac{k}{\rho C_p}\nabla^2 T + \frac{Q}{\rho C_p} \tag{3}$$

These equations are discretized by MPS method as moving particles and calculated by semi-implicit way. The equation (3) is calculated explicitly.

2.2 Particle interaction models

In the MPS method, the weight function and particle interaction models corresponding to each differential operator are usually used. The weight function *w(r)* makes particles interact with only near ones in the influence radius of r_e. The weight interactions depend on a distance between two particles as a shorter distance interacts strongly as follows:

$$w(r) = \begin{cases} \dfrac{r_e}{r} - 1 & (0 \le r < r_e) \\ 0 & (r_e \le r) \end{cases} \tag{4}$$

Gradient and laplacian model of quantities ϕ are discretized with following equations respectively:

$$\langle \nabla \phi \rangle_i = \frac{d}{n^0} \sum_{j \neq i} \frac{(\phi_j - \phi_i)(\boldsymbol{r_j} - \boldsymbol{r_i})}{|\boldsymbol{r_j} - \boldsymbol{r_i}|^2} (\boldsymbol{r_j} - \boldsymbol{r_i}) w_{ij} \tag{5}$$

$$\langle \boldsymbol{\nabla}^2 \phi \rangle_i = \frac{2d}{\lambda n^0} \sum_{j \neq i} (\phi_j - \phi_i)\, w_{ij} \tag{6}$$

Where w_{ij} , d, n^0 are the value of the weight function between two particles i and j, the number of the space dimension, and the constant value of particle number density for incompressible condition, respectively. The particle number density is defined as follows:

$$n_i = \sum_{j \neq i} w_{ij} \tag{7}$$

And λ is the parameter to confirm a dispersion of quantities distribution to analysis solution and as follows:

$$\lambda = \frac{\sum_{j \neq i} |\boldsymbol{r_j} - \boldsymbol{r_i}|^2 w_{ij}}{\sum_{j \neq i} w_{ij}} \tag{8}$$

2.3 Thermal field calculation model

Equation (3) is discretized with equation (6) as follows:

$$T_i^{k+1} = T_i^k + \frac{\Delta t}{\rho C_p} \frac{2d}{\lambda n^0} \sum_{j \neq i} \frac{2k_i k_j}{k_i + k_j} \left(T_j^k - T_i^k\right) w_{ij} + \frac{Q}{\rho C_p} \tag{9}$$

Where the reason for using harmonic mean of heat conductivity between two particles i and j is to replicate the heat transfer between two different bodies.

Buoyancy by different temperature and density is modeled with the Boussinesq approximation. The external volume force $\boldsymbol{F}$ in equation (2) is expressed by the buoyancy force

$$\boldsymbol{F} = \beta \boldsymbol{g} (T - T_r) \tag{10}$$

Where $\boldsymbol{g}$ is the acceleration due to gravity, T_r is the reference temperature that is equal to the average value of the top and bottom temperature, and β is the thermal expansion coefficient.

In the case that phase transition and temperature change occur at the same time such as mixtures, viscosity is modeled to depend on the temperature change exponentially in the phase transition area. Particularly temperature dependency of viscosity is dealt with the following Ramaccotti equation [6]:

$$\nu(T) = \nu_L \exp(2.5 \cdot C \cdot f) \tag{11}$$

Where ν_L is the kinematic viscosity in liquid phase. In fact, real core melt might have temperature dependence of viscosity in the liquid area, but it is very small compared with the value in the phase change area. So it is regarded as a constant value. C is the constant value

between, generally, 4 and 8. For the present analysis C is shown in **Table1-4**. f is the solid fraction which is assumed to changed linearly in the area. When the solid fraction of a particle is over a constant value (i.e. 1.0), the particle change into solid from liquid. A solid particle is assumed to have a constant value of kinematic viscosity. A kinematic viscosity between two different particles is given by harmonic mean.

2.4 Improved calculation model for spreading

When treating high temperature melts, radiation heat transfer from surface is important phenomenon. In the MPS method, radiation heat transfer is simply modeled as heat removal from free surface particles. The radiation heat removal is based on Stefan-Boltzman's law. Calculated radiation amount is converted to temperature decrease as follow:

$$\Delta T_i = \frac{\varepsilon \sigma A T_i^4}{\rho C_p {l_0}^3} \Delta t \tag{12}$$

Where ε is the radiation rate, σ is the Stefan-Boltzman constant, A is the surface area of a particle i and l_0 is the initial distance between particles. The radiation rate should be a value considering an environment, instead of the real radiation rate. It means, for examples, that in the case an experiment conducted in an enclosed region the radiation rate is used 0.2-0.5. Free surface area of particle i depends on the particle number density such as:

$$A = \left(1 - \frac{n_i}{n_0}\right) 2d{l_0}^3 \tag{12}$$

Additionally, the analysis of the spreading behavior with solidification needs to treat high viscosity materials as a result of solidification. It means that explicit calculation of the viscous term in the original MPS method takes a long time to calculate for numerical stability. In the present study, the viscous term was calculated implicitly and limitation of time step is ignored. The viscous term is discretized with equation (6) as follow:

$$\boldsymbol{u}_i^{k+1} = \boldsymbol{u}_i^k + \Delta t \frac{2d}{\lambda n^0} \sum_{j \neq i} \left(\boldsymbol{u}_j^{k+1} - \boldsymbol{u}_i^{k+1}\right) w_{ij} \tag{13}$$

Simultaneous equation about Equation (13) is solved with the conjugated gradient (CG) method with preprocessing of diagonal scaling.

In the MPS method, the pressure calculation is done with a temporary position calculated by the external volume force and viscous term. However, if a relative velocity between two particles is very large, the value of the weight function become larger than real pressure and occur numerical instability in the pressure gradient term. To overcome the problem, the original MPS method generally relaxes the impossibly large momentum variation. Before the pressure calculation, the momentum of two particles near in a threshold value r_c is relaxed with a parameter C. The relaxed velocity $\boldsymbol{u}'_{i,c}$ of a particle i is decided as follow:

$$\boldsymbol{u}'_{i,c} = (1 + C) \frac{1}{m_i} \cdot \frac{m_i m_j}{m_i + m_j} \cdot \frac{\min(0, (u_j{}^* - u_i{}^*) \cdot (\boldsymbol{r}_j{}^* - \boldsymbol{r}_i{}^*))}{\left|\boldsymbol{r}_j{}^* - \boldsymbol{r}_i{}^*\right|^2} \tag{14}$$

One of a particle j is calculated based on the law of action and reaction. In the present study, 0.8 l_0 and 0.5 are used for r_c and C respectively.

3 FARO EXPERIMENT ANALYSIS

Based on the improved MPS method, the FARO L26S experiment was analyzed. The experiment used a mixture of UO_2 and ZrO_2 (mass fraction 80:20) simulating high temperature core melt. The mixture was dropped to the floor of stainless steel and its spreading behavior with solidification was observed.

3.1 Analysis condition

Figure1 is the analysis model. The particle size was 2cm, the influence radius r_e was $2.1l_0$ and fluid particle number was 2496. Almost fluid particles flow down to the floor until first 10 seconds. The melt was heated up at the top, kept temperatures of 2950K and phase transition area was from 2860K to 2910K. The initial floor temperature was 290K. **Table1** shows the physical property of the melt and floor. The radiation rate used 0.5 to simulate enclosed region of the FARO experiment.

Table 1: the property in the FARO L26S [1]

Melt	
Initial temperature	2950(K)
Solid fraction changing phase	1.0
Density	8000(kg/m^3)
Specific heat	500(J/kgK)
Heat conductivity	3.0(W/mK)
Dynamic viscosity(2910K)	0.005(Pa s)
Parameter C in the Ramaccotti model	5.77
Stainless floor	
Initial temperature	290(K)
Density	8000(kg/m^3)
Specific heat	499(J/kgK)
Heat conductivity	30.0(W/mK)

3.2 Results and discussions

Figure 2 shows the solidification morphology at 2s and 6s. In **Figure2,** the left side shows the results by Kawahara and the right side shows the present results [5]. Compared with the result of previous study, the improved method suppressed particles dispersion when the melt flow down. So the quantity of the melt was not decreased and the leading edge of the melt was sharp shape.

The leading edge position of the melt was compared with the experiment and the previous calculation in **Figure3.** Solid lines in this figure indicate the leading edge for the different lateral positions of the experiment. Experimental result shows a clear multistage curve. During the spreading, leading edge of melt stopped twice (2-4s and 7-9s). These spreading stops were caused by a crust formation by temperature decrease at the edge of the melt. The crust made the spreading slow and after that, melt coming from the behind went over. Although the THEMA code could not simulate well such spreading stop of the crust formation like stair, MPS calculation simulated the step formation, but its time did not agree with the experimental result [7].

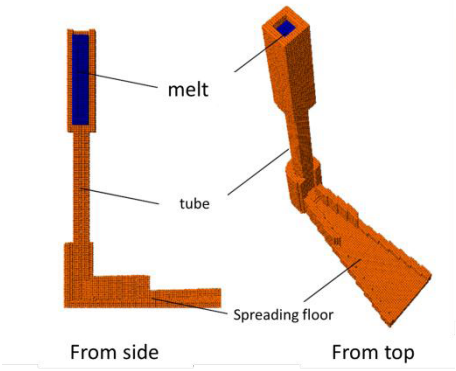

Figure 1: MPS analysis model for FARO

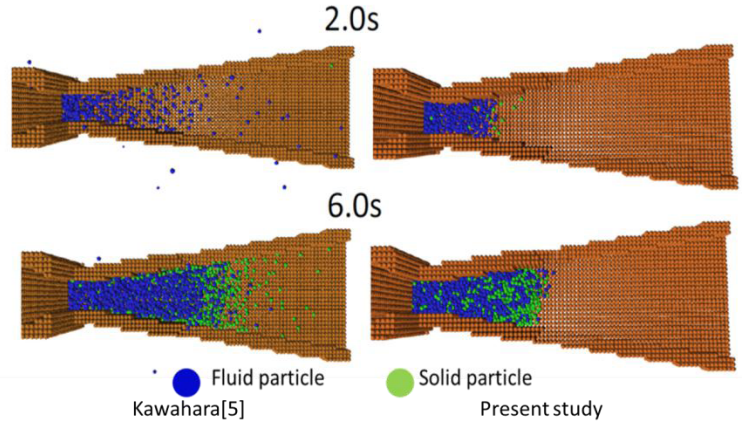

Figure 2: MPS calculation reslut for FARO[5]

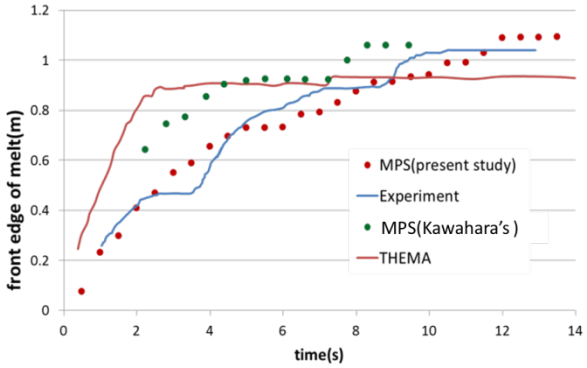

Figure 3: front edge of melt for FARO [5,7]

4 ECOKATS-V1 EXPERIMENT ANALYSIS

This experiment was one of the ECOSTAR project experiments which utilized oxide mixture melt [8]. The high temperature melt was kept in the tank on the upper place and flowed down to the liner ceramic floor, which was the length of 8m. The pit under the tank stored the fallen melt temporarily. The melt weight was 300kg and composed of Al_2O_3(41%), FeO(24%), CaO(19%) and SiO_2(16%). In the experiment, the melt was temporarily stored in the pit and flowed to the ceramic floor. Finally the melt of 193kg was on the floor. The experiment was conducted out of doors.

4.1 Analysis condition

Figure4 shows the analysis model for MPS calculation in two dimensions. This is because the channel of the experiment was liner. Particle size was 5mm, the number of fluid particles was 12240 and the length of the floor was 10m. **Table2** shows the physical property of the melt and floor, which is same property used in the analysis by Farmer [7].

Table 2: the property in the ECOKATS-V1

Melt	
Initial temperature	1860(K)
Solid fraction changing phase	1.0
Density	3263(kg/m^3)
Specific heat	1220(J/kgK)
Heat conductivity	5.4(W/mK)
Dynamic viscosity(1822K)	0.2(Pa s)
Parameter C in the Ramaccotti model	1.8
Radiation rate	0.95
Phase change area	1373-1822(K)
Ceramic floor	
Initial temperature	276(K)
Density	2200(kg/m^3)
Specific heat	840(J/kgK)
Heat conductivity	3.8(W/mK)

4.2 Results and discussions

Figure5 shows the change of the front edge of the melt with time by MPS calculation. The result showed good agreement with the experimental result. The final position of melt also accurately agreed. In the experiment, the melt spread step by step like the FARO experiment. In MPS calculation, the step-like spreading behavior was observed at 50sec and 70sec.

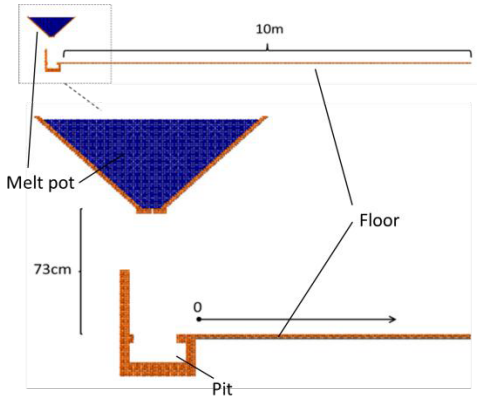

Figure 4: MPS analysis model for ECOKATS-V1

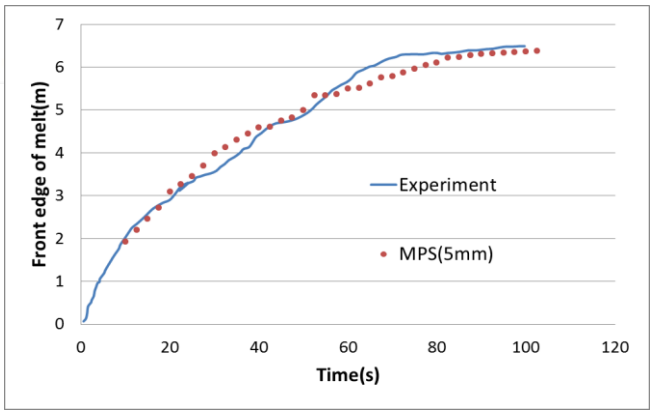

Figure 5: front edge of melt for ECOKATS-V1 [8]

5 WATER SPREADING TEST BY THEOFANOUS

This experiment was conducted by Theofanous et al. [9]. and simulated a pedestal floor of BWR Mark I containments. A scale of the experiment was one tenth of the real scale. The center part is the water inflow area shown in **Figure6**. Firstly water flowed in the area surrounded by the inner wall with the diameter of 56.6cm, and flowed out a channel between the inner and outer wall with the diameter of 113cm. Water flowed at flow rate of 0.325kg/min and a spreading area was measured. The experiment was used for validation of the Debris Spreading Analysis (DSA) module in the severe accident analysis code,

SAMPSON, in Japan. The result of MPS calculation could be compared with the one by DSA calculation.

5.1 Analysis condition

Figure6 shows the analysis model for MPS calculation. Particle size was 5mm and the influence radius was $2.1l_0$. **Table3** shows physical property of water and concrete floor. Inflow boundary was at the center and flow rate was 0.325kg/min.

Table 3: the property in the Theofanous water spreading test

Water	
Density	1000(kg/m^3)
Kinematic viscosity	1.0×10^{-6}(m^2/s)
Concrete floor	
Density	2300(kg/m^3)

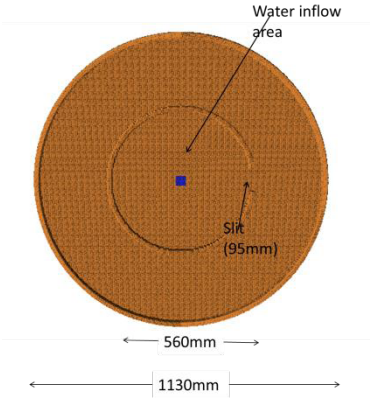

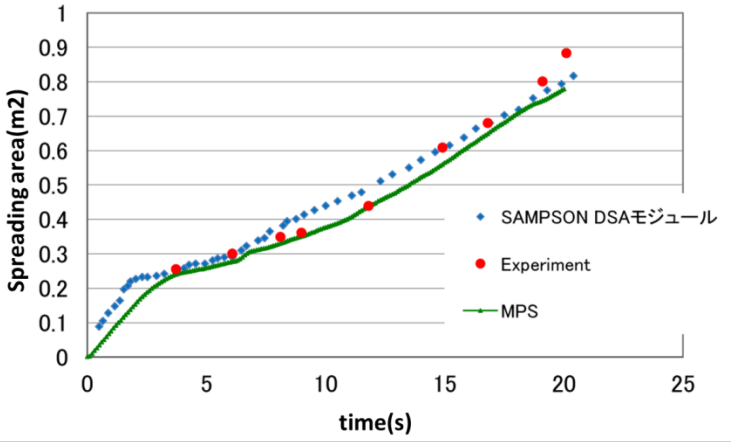

Figure 6: MPS analysis model for water spreading test **Figure 7**: Spreading area for water spreading test [9]

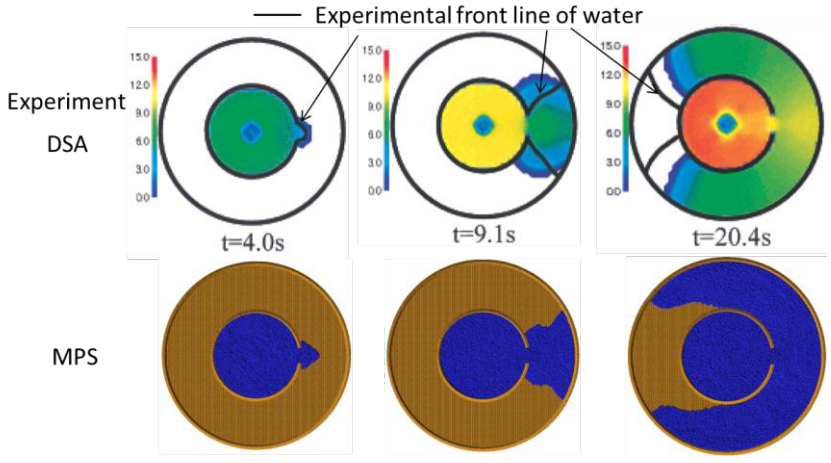

Figure 8: Spreading area for water spreading test [9]

5.2 Results and discussions

As a result, change of spreading area with time is shown in **Figure7**. In 0sec to 18sec, MPS calculation result agreed with the experimental result. Both MPS and DSA calculation after 18sec do not agree with the experiment. **Figure8** shows the experimental result and calculation results of DSA and MPS. DSA and MPS calculation gave almost same result for isothermal water spreading analysis.

6 SPREAD TEST ANALYSIS

These tests involved spreading of stainless steel melts in test sections that mimicked the key features of the GE BWR Mark I containment. Particularly melt was poured into a cylindrical cavity that represented the reactor pedestal. The melt then spread into a large open region simulating the cavity annulus through a doorway. Although many spreading tests were conducted in this program, minimal data was reported in the open literature. Test number 15 had sufficient information and was a dry cavity experiment. The experiment was used for validation of the DSA module in the SAMPSON code. The result of MPS calculation with solidification was compared with the DSA calculation.

6.1 Analysis condition

Figure9 shows the analysis model for MPS calculation. The diameter of the cylindrical cavity was 35cm. The total weight of the melt was 63.6kg and initial temperature was 1804K. The melt was fully fell down from the melt pot at the top in 6.7sec. The particle size was 1cm and the influence radius was $2.1l_0$. **Table4** shows physical property of stainless steel melt and concrete floor [7].

Table 4: the property in the SPREAD test

Melt of stainless steel	
Initial temperature	1804(K)
Solid fraction changing phase	1.0
Density	6820(kg/m^3)
Specific heat	560(J/kgK)
Heat conductivity	20.0(W/mK)
Dynamic viscosity(1822K)	0.002(Pa s)
Parameter C in the Ramaccotti model	7.26
Radiation rate	0.8
Phase change area	1671-1727(K)
Concrete floor	
Initial temperature	298(K)
Density	2300(kg/m^3)
Specific heat	1670(J/kgK)
Heat conductivity	1.3(W/mK)

6.2 Results and discussions

As a result, spreading area is shown in **Figure10** [10]. The experimental result was given only final spreading area, and it is shown as constant value in **Figure10**. MPS calculation showed agreement with the experimental result for final spreading area. Compared with the DSA calculation, the melt spread rapidly in MPS. **Figure11** shows the final states of the melt when spreading stopped at 25sec. MPS result was overspread for the leading edge. The experimental result for leading edge of the melt was 0.91 m and MPS result was 1.17 m [7]. The detail of stainless melt spreading experiment was not reported. The DSA calculation was stopped in liquid phase and solidified [10]. The melt spreading in MPS was stopped by solidification at the leading edge. This was a main difference between DSA and MPS simulation with high temperature melt and heat transfer calculation.

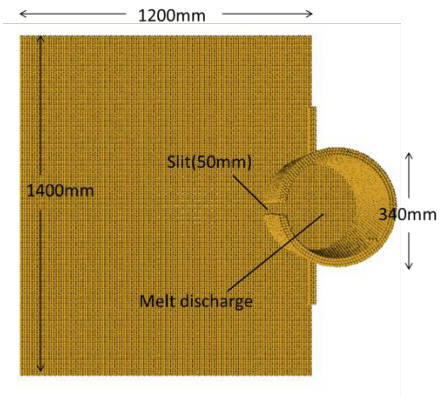

Figure9: MPS analysis model for SPREAD

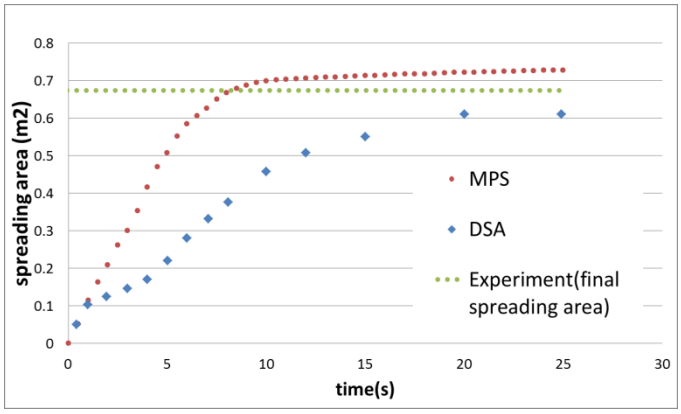

Figure10: spreading area of stainless melt for SPREAD [10]

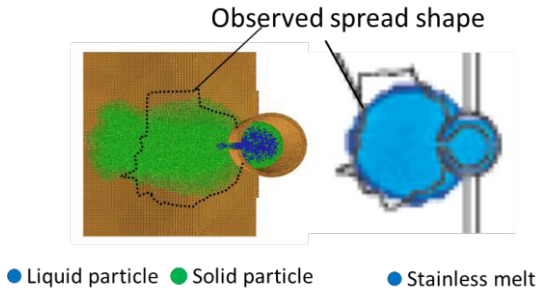

Figure11: final states of melt spread(25sec) [10]

7 CONCLUSIONS

- The MPS method was improved for analysis of the spreading behavior with solidification to calculate radiation heat transfer based on the surface area depending on particle number density. The viscous term was calculated implicitly for high viscosity materials, which made calculation faster with numerical stability.
- Based on the improved MPS method, the FARO L26S and ECOKATS-V1 experiment were analyzed. The results showed good agreements with the experimental result for the leading edge of the melt. The tendency to spread stopping

caused by crust formation at the front edge was simulated by MPS.
- The water spreading experiment by Theofanous was analyzed by MPS and SAMPSON DSA calculation. Both agreed with the experiment.
- SPREAD test using stainless steel melt is analyzed by MPS. MPS calculation agreed with the final spreading area. Change of spreading area with time did not agree between MPS and DSA module of the SAMPSON code.
- The MPS method will be useful for computer experiments with various physical property of corium. It is expected to improve severe accident analysis code.

ACKNOWLEDGEMENT

This work has been financially supported by the Japanese government's Ministry of Economy, Trade, and Industry. Technical support from the project team is greatly appreciated.

The MPS code of the present study was developed based on MPS-SW-MAIN-Ver.2.0 which was kindly provided by Koshizuka and Shibata [11].

REFERENCES

[1] W.Tromm, A.Fushimi and J.J.Foit, "Dry and wet spreading experiments with prototypic material at the FARO facility and theoretical analysis." , proceedings of OECD Workshop on Ex-Vessel Debris Coolability Karlsruhe Germany, 15-18 November 1999.

[2] J J Foit, A. Veser, "Simularity solutions for non-isothermal spreading. KATS experiments and CORFLOW results," *7th International Conference on Nuclear Engineering*., Tokyo, Japan, 19-23, April, 1999, ICONE-7036 , 1999.

[3] B. Spindler, J. M. Veteau, "The simulation of melt spreading with THEMA code Part 2: Assessment against spreading experiments", Nuclear Engineering and Design, 236, 425-441, 2006.

[4] S. Koshizuka, Y. Oka, "Moving –particle semi-implicit method for fragmentation of incompressible fluid," *Nuclear Science and Engineering*., **123**, 421-434 (1996).

[5] T.Kawahara, Y.Oka: "Ex-Vessel molten core solidification behavior by moving particle semi-implicit method" , J. Nucl. Sci. Technol, Vol.49 No.12, pp1156-1164, 2012.

[6] G. Cognet, F. Sudreau, M. Ramacciotti, C. Journeau and J.M. Seiler: Methodology for Corium-Concrete Viscosity Calculations. In H. Alsmeyer (editor): Proceedings of the OECD Workshop on Ex-Vessel Debris Coolability, p.408–420. Forschungszentrum Karlsruhe, 2000. FZKA 6475.

[7] M.T.Famer, "Melt Spreading Code Assessment, Modications, and Applications to the EPR Core Catcher Design", Nuclear Engineering Division, Argonne National Laboratory, March,2009.

[8] H. Alsmeyer et al,"Test Report of the Melt Spreading Tests ECOKATS-V1 and ECOKATS-1", ECOSTAR, Fifth Framework Program, 1998-2002.

[9] Masataka HIDAKA, Hiroshi UJITA, "Verication for Flow Analysis Capability in the Model of Three-Dimensional Natural Convection with Simultaneous Spreading, Melting and Solidication for the Debris Coolability Analysus Module in the Severe Accident Analysis Code'SAMPSON'(I) ", J. Nucl. Sci. Technol, Vol38, No.9, p.745-756, September , 2001.

[10] Masataka HIDAKA, Hiroshi UJITA, "Verication for Flow Analysis Capability in the

Model of Three-Dimensional Natural Convection with Simultaneous Spreading, Melting and Solidication for the Debris Coolability Analysus Module in the Severe Accident Analysis Code'SAMPSON'(II) ", J. Nucl. Sci. Technol, Vol39, No.5, p.520-530, May , 2002.

[11] S.Koshizuka, K.Shibata, "MPS-SW-MAIN-Ver.2.0", P 8827-1, 23 Feburary, 2006.